# Skeletal muscle fuel utilisation in healthy and disregulated states

**Problem presented by**

Dr Laura Pickersgill

*Unilever Corporate Research*

and

Prof Ian MacDonald

*University of Nottingham*

## Problem statement

In healthy lean subjects, skeletal muscle displays metabolic flexibility, that is, it is capable of switching between predominantly lipid oxidation with high rates of fatty acid uptake during fasting conditions, and the suppression of lipid oxidation in favour of increased glucose uptake, oxidation and storage in response to insulin during the fed state. Insulin resistant states such as obesity and Type 2 diabetes are characterised by this loss of, or reduction in, fuel-switching ability. The aim is to develop a mathematical model of skeletal muscle fuel utilisation, that will enable an investigation of the dynamics of skeletal muscle glucose and lipid handling in response to a meal, as well as the effects of insulin on these dynamics.

## Study Group contributors

Helen Byrne (University of Nottingham)
Poul Hjorth (Technical University of Denmark)
John King (University of Nottingham)
Anthony Lock (University of Oxford)
Tobias Locsei (University of Cambridge)
Nick McCullen (University of Bath)
Joanne Miller (University of Nottingham)
Ashley Pitcher (University of Oxford)
John Ward (Loughborough University)
Jonathan Wattis (University of Nottingham)

## Report prepared by

Jonathan Wattis (University of Nottingham)

# 1   Introduction

The average human diet consists of a combination of carbohydrates (50%) and lipids (fats, 30%), delivered as meals in a discontinuous manner. Human physiology has evolved mechanisms that enable it to cope with discontinuities in the supply of and the demand for energy. In the healthy state, the organs respond to plasma (blood) nutrient levels through a series of well-controlled mechanisms, such that energy is stored at times of surplus and is released at times of requirement. Efficient handling of post-prandial nutrients results in a minimal glucose response, appropriate insulin secretion, suppression of stored lipid mobilization and oxidation, along with activation of energy uptake into tissues for storage. Thus healthy carbohydrate and lipid metabolism is dependent upon the coordinated regulation of the organs governing carbohydrate and lipid fluxes, namely the brain, pancreas, liver, skeletal muscle and adipose tissue.

In lean, healthy individuals there is a high reliance upon lipid oxidation with high rates of fatty acid uptake during fasting conditions. In addition healthy tissue displays metabolic flexibility, that is, it is capable of switching between lipid oxidation in the fasted state and the suppression of lipid oxidation in favour of increased glucose uptake, oxidation and storage during the fed state [2]. In obese subjects, there is a lesser reliance on lipid and a greater reliance on glucose oxidation in both the fed and the fasted states.

This reduction in the ability to switch between fuel types in obese subjects is characteristic of insulin resistant states such as obesity and Type 2 diabetes [6]. Subjects with such conditions exhibit failure to increase lipid oxidation in the fasted state and failure to suppress lipid oxidation in response to increased insulin levels.

In skeletal muscle of a lean, healthy individual, insulin strongly suppresses lipid oxidation during insulin-stimulated (fed) conditions and induces a high reliance upon glucose oxidation, whereas in skeletal muscle of an obese, insulin resistant individual, there is less stimulation of glucose oxidation by insulin and blunted suppression of lipid oxidation. Thus, in the skeletal muscle of obese, insulin resistant individuals, there is a constricted range in switching between lipid and glucose oxidation compared to the dynamic switching observed in lean, healthy individuals. This constrained homeostatic adjustment to the transitions between fasting and insulin-stimulated conditions in obese, insulin resistant individuals has been described as 'metabolic inflexibility' of skeletal muscle [13, 7].

We aim to develop a mathematical model of skeletal muscle fuel utilization, that will enable an investigation of the dynamics of skeletal muscle glucose and lipid handling in response to a meal. The model should:

- initially aim to reproduce data that describe the effect of an individual's fat mass and insulin sensitivity on the preference for fat/glucose oxidation in myocytes (metabolic flexibility of muscle cells);

- aim to simulate the effects of different rates of delivery of glucose and lipid to skeletal muscle in the fed and fasted states;

- allow us to investigate the effects of varying glucose and fatty acid availability on preference for fat oxidation in individuals with different phenotypes (varied body mass index, fat mass and insulin sensitivity).

In Section 2, we construct a model of a muscle cell, including

- the transport of glucose and lipids from the blood stream into the cells,
- the cell's internal storage of glucose as glycogen, and
- the glucose and lipid oxidation processes.

We show that the system has a physically-relevant steady-state solution (Section 2.2). When nondimensionalising the model (Section 2.3) to make the numerical solutions more straightforward we obtain a number of constraints on the relative sizes of parameter groups (Section 2.4). Section 3 contains a description of the results of our numerical solutions, and conclusions are drawn in Section 4.

# 2  Metabolism

The metabolic system is complicated and involved. For the purposes of the problem to be studied herein, it is not necessary (nor, indeed, is it helpful) to consider all the interactions known. Therefore we consider a simplified system (shown in Figure 1).

The main currency of energy in cells is adenosine triphosphate (ATP). Energy is released from ATP upon removal of a phosphate from ATP, forming ADP (adenosine diphosphate) via the enzyme-mediated reaction

$$ATP + H_2O \rightarrow ADP + HPO_4 + \Delta E, \tag{1}$$
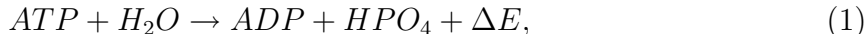
where $\Delta E$ denotes the amount of energy released, and $HPO_4$ is the phosphate group removed from ATP. A second phosphate group can be lost from ADP, yielding adenosine monophosphate (AMP) and releasing further energy. To avoid energy depletion, cells need to activate processes which take fuel into cells and convert AMP and ADP to ATP. The processes of glucose and fat oxidation produce ATP. It is the purpose of this report to investigate the interaction between these two ATP resynthesising, fuel oxidation pathways. For simplicity, we focus on AMP, and its conversion to ATP, and we denote by $P$ the concentration of a chemical species which controls the activity of this pathway. By 'activity' we mean the flux of material through the pathway. We expect $P$ to be strongly correlated with the concentration of AMP. The simplest option is to simply take $P$ as the concentration of AMP; however, future work may identify an enzyme which more conveniently describes the activity of the AMP $\mapsto$ ATP pathway. The variable $P$ will be large when muscle cells have recently done work and, as cells recover and replenish their ATP levels, $P$ will decrease. We are interested in the whole process from feeding through digestion of an (evening) meal, to the fasted state which is typically reached about 12 hours later.
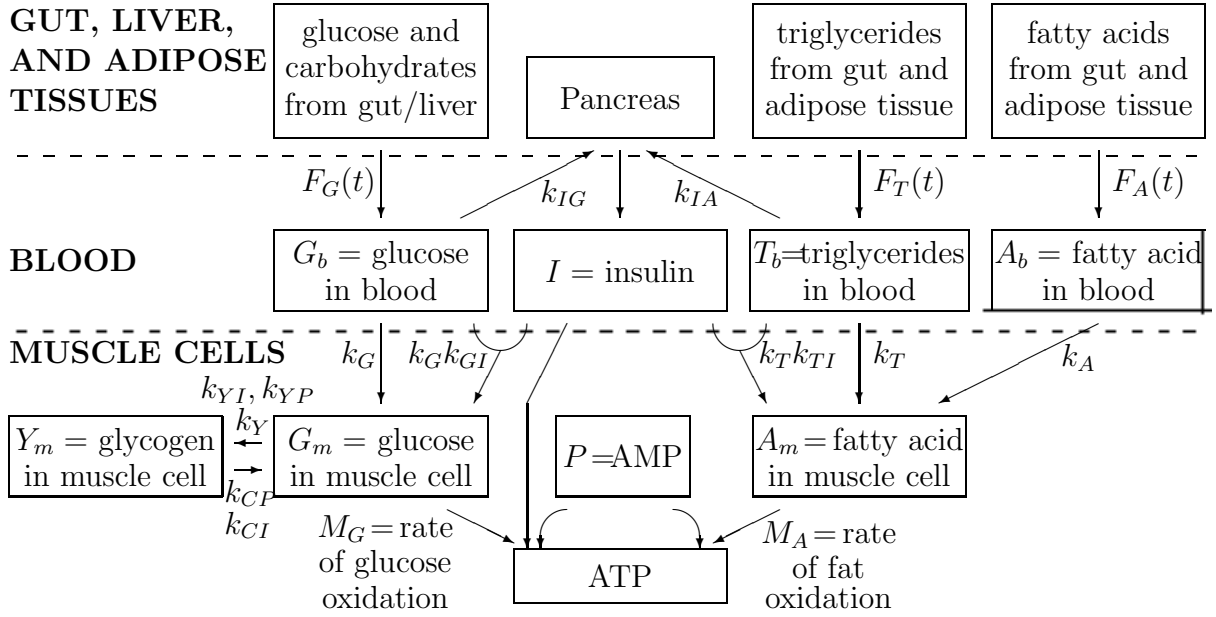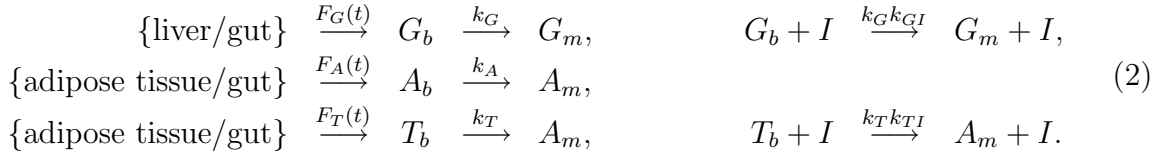
Figure 1: Diagram of the biochemical reaction network modelled in the rest of this paper.

## 2.1 The model

We construct a compartmental model of the system illustrated in Figure 1 by formulating ordinary differential equations for the spatially-averaged concentrations of glucose, glycogen, insulin, free fatty acids (FFA) and triglycerides (TG), both systemically (in the blood supply) and the muscle cells.

The processes included in Figure 1 can be represented by the chemical processes

$$
\begin{aligned}
\{\text{liver/gut}\} &\quad \xrightarrow{F_G(t)} \quad G_b \quad \xrightarrow{k_G} \quad G_m, &\quad G_b + I \quad \xrightarrow{k_G k_{GI}} \quad G_m + I, \\
\{\text{adipose tissue/gut}\} &\quad \xrightarrow{F_A(t)} \quad A_b \quad \xrightarrow{k_A} \quad A_m, &\quad \\
\{\text{adipose tissue/gut}\} &\quad \xrightarrow{F_T(t)} \quad T_b \quad \xrightarrow{k_T} \quad A_m, &\quad T_b + I \quad \xrightarrow{k_T k_{TI}} \quad A_m + I.
\end{aligned}
\tag{2}
$$

These represent the transport of glucose, free fatty acids and triglycerides from the gut, liver and adipose tissue through the blood plasma to muscle cells. Some processes are 'passive' in that they simply rely on concentration gradients, and have rates denoted by $F_G$, $k_G$, *etc.*; other processes are accelerated by the presence of hormones, such as insulin ($I$): these are denoted by acceleration factors $k_{GI}$ and $k_{TI}$.

Once inside the cell, glucose can be stored as glycogen, which we denote by the chemical process $G_m \rightleftharpoons Y_m$. To make this apparently simple process more realistic we make the storage and release rates depend both on the insulin concentration ($I$) and the amount of work done recently by cells (which we assume can be described by $P$). Hence

$$
G_m \quad \rightharpoonup \quad Y_m \qquad \text{rate} \; = k_Y \left( \frac{1 + k_{YI}I}{1 + k_{YP}P} \right),
\tag{3}
$$

$$
G_m \quad \leftharpoonup \quad Y_m \qquad \text{rate} \; = \frac{k_{CP}P}{1 + k_{CI}I}.
\tag{4}
$$

Finally, we describe the oxidation of glucose and fatty acids. We assume the former occurs only in the presence of insulin, but then occurs rapidly (insulin acting as a catalyst), while the latter occurs more slowly, but does not require a catalyst, that is

$$P + G_m + I \xrightarrow{M_G} ATP + I, \tag{5}$$

$$P + A_m \xrightarrow{M_A} ATP. \tag{6}$$
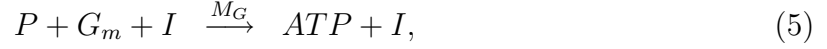
We model the flow of the nutrients (glucose, fatty acids and triglycerides) into the blood stream by the functions

$$F_G(t) = \beta_G + \frac{F\theta_G t}{B_G^2} e^{-t^2/2B_G^2}, \tag{7}$$

$$F_A(t) = \beta_A + \frac{F\theta_A t}{B_A^2} e^{-t^2/B_A^2}, \tag{8}$$

$$F_T(t) = \beta_T + \frac{F\theta_T t}{B_T^2} e^{-t^2/B_T^2}, \tag{9}$$

which will appear as 'forcing' terms in differential equations derived later. These functions have the form of a linear growth followed by a smooth peak and rapid decay. The position of the maximum and total area under the curve can be varied by judicious choice of $B_*$ and $\theta_*$. Here, the $B_*$ parameters denote the rate at which the nutrients are released from a meal, the parameters $\theta_*$ describe the relative proportion, in a diet, of each type of nutrient, and $F$ is a measure of the total diet, such that $F\theta_G$ is a glucose concentration, and $F\theta_A$ and $F\theta_T$ are fat concentrations. The $\beta_*$ parameters denote a background (basal) rate of supply to the blood stream from the liver and from adipose tissue.

The functions (7)–(9) are inputs to the equations governing the concentrations of glucose, $G_b$, free fatty acids, $A_b$, and triglycerides, $T_b$, in the blood plasma:

$$\underbrace{\alpha \frac{dG_b}{dt}}_{\substack{\text{rate of change of} \\ \text{blood glucose conc.}}} = \underbrace{F_G(t)}_{\substack{\text{source of} \\ \text{glucose from} \\ \text{gut \& liver}}} - \underbrace{S_G G_b}_{\substack{\text{use of glucose} \\ \text{by rest of} \\ \text{body}}} - \underbrace{k_G(1 + k_{GI}I)G_b,}_{\substack{\text{uptake of glucose} \\ \text{by muscle cells (incl.} \\ \text{control by insulin)}}} \tag{10}$$

$$\underbrace{\alpha \frac{dA_b}{dt}}_{\substack{\text{rate of change} \\ \text{of blood fatty} \\ \text{acid conc.}}} = \underbrace{F_A(t)}_{\substack{\text{source of fatty} \\ \text{acids from gut} \\ \text{\& adipose tissue}}} - \underbrace{S_A A_b}_{\substack{\text{use of fatty acids} \\ \text{by rest of body}}} - \underbrace{k_A A_b,}_{\substack{\text{uptake of} \\ \text{fatty acids by} \\ \text{muscle cells}}} \tag{11}$$

$$\underbrace{\alpha \frac{dT_b}{dt}}_{\substack{\text{rate of change} \\ \text{of blood} \\ \text{triglyceride conc.}}} = \underbrace{F_T(t)}_{\substack{\text{source of} \\ \text{triglycerides from} \\ \text{gut \& adipose tissue}}} - \underbrace{S_T T_b}_{\substack{\text{use of} \\ \text{triglycerides by} \\ \text{rest of body}}} - \underbrace{k_T(1 + k_{TI}I)T_b.}_{\substack{\text{uptake of} \\ \text{triglycerides by} \\ \text{muscle cells}}} \tag{12}$$

We assume that each nutrient is utilised by other tissues in the body, at rates $S_G$, $S_A$, $S_T$, as well as being transported into muscle cells as shown in Figure (1) at rates $k_G$, $k_A$, $k_T$.

We introduce the parameter $\alpha$ which is defined as the ratio of the blood volume to the muscle volume. Due to $G_b$ and $G_m$ both being concentrations, and the blood volume being less than the muscle volume, as molecules cross from the plasma into muscle cells the decrease in concentrations in the blood volume is greater than the increase in the muscle volume. Similar differences occur between $A_b$ and $A_m$, and $T_b$ and $A_m$.

Whilst fatty acids cross into cells passively, the transport of glucose is controlled by insulin, and that of triglycerides is more complex still. Triglycerides (TG) are first converted into fatty acids in an enzyme-catalyzed reaction prior to being taken up into cells. For simplicity, we assume that insulin controls this process, whereas in reality there is some debate as to the importance of insulin/other hormones in the uptake of plasma TG into skeletal muscle. In later work we aim to investigate the evidence for the control of TG uptake and to describe this pathway in more detail by modelling how blood TG concentration depends on diet, and insulin, *etc.* The insulin-dependencies are denoted by the constants $k_{GI}$ and $k_{TI}$. It is known that insulin controls the uptake of triglycerides into some cells in the human body, but it has not yet been confirmed that it is the controlling hormone for triglyceride uptake by muscle cells. The enzyme lipoprotein lipase regulates the uptake of triglycerides into muscle cells, and this is controlled by some hormone, which we postulate to be insulin, and hence introduce the rate parameter $k_{TI}$. Later, we can assume that insulin is not involved, and so put $k_{TI} = 0$.

The insulin concentration is governed by the concentrations of glucose and fatty acids in the blood, along with a rate of decay, $\lambda_I$; its concentration is determined from

$$\underbrace{\frac{\mathrm{d}I}{\mathrm{d}t}}_{\substack{\text{rate of change} \\ \text{of blood} \\ \text{insulin conc.}}} = \underbrace{k_{IG}G_b}_{\substack{\text{creation of} \\ \text{insulin due to} \\ \text{blood glucose}}} + \underbrace{k_{IA}A_b}_{\substack{\text{creation of} \\ \text{insulin due to} \\ \text{blood fatty acids}}} - \underbrace{\lambda_I I.}_{\substack{\text{natural decay} \\ \text{of insulin}}} \tag{13}$$

Inside muscle cells, glucose can be converted into glycogen – a short-term energy store, which we denote by $Y_m$. This process is controlled by insulin, $I$, which binds to receptors on the surface of muscle cells and can thence influence processes occurring inside the cells. Furthermore, we assume that the reversible conversion of glucose to glycogen is influenced by the chemical species we denote by $P$, which is strongly correlated to the concentration of AMP.

We assume that $P$ is created by physical activity at a rate $\mu$, and is degraded naturally at some rate $\lambda_P$; the dynamics we are primarily interested in are the switching between the oxidation of $P$ by glucose and by fatty acids, and how the switch between the two occurs. We assume that glucose oxidation occurs rapidly in the presence of insulin and $P$. Although enzymes do regulate fatty acid oxidation, we do not detail them here; instead we assume that no enzyme is required to activate this process, and that fatty acid oxidation occurs slowly in the presence of $P$. The rates of the glucose and fatty acid oxidation processes are denoted $M_G$ and $M_A$ respectively; $\gamma_g$ and $\gamma_a$ are the number of $P$ molecules used in the oxidation of a glucose and a fatty acid molecule respectively.

The concentrations in muscle cells evolve according to

$$\underbrace{\frac{dG_m}{dt}}_{\substack{\text{rate of change} \\ \text{of muscle} \\ \text{glucose conc.}}} = \underbrace{k_G(1 + k_{GI}I)G_b}_{\substack{\text{insulin-controlled uptake} \\ \text{of glucose into muscle cells}}} - \underbrace{M_G P I G_m}_{\substack{\text{insulin-mediated} \\ \text{oxidation of glucose}}}$$

$$- \underbrace{k_Y\left(\frac{1 + k_{YI}I}{1 + k_{YP}P}\right)G_m}_{\substack{\text{storage of glucose} \\ \text{as glycogen}}} + \underbrace{\frac{k_{CP}PY_m}{1 + k_{CI}I}}_{\substack{\text{conversion of glycogen} \\ \text{back into glucose}}}, \tag{14}$$

$$\underbrace{\frac{dY_m}{dt}}_{\substack{\text{rate of change} \\ \text{of muscle} \\ \text{glycogen conc.}}} = \underbrace{k_Y\left(\frac{1 + k_{YI}I}{1 + k_{YP}P}\right)G_m}_{\substack{\text{storage of glucose} \\ \text{as glycogen}}} - \underbrace{\frac{k_{CP}PY_m}{1 + k_{CI}I}}_{\substack{\text{conversion of glycogen} \\ \text{back into glucose}}}, \tag{15}$$

$$\underbrace{\frac{dA_m}{dt}}_{\substack{\text{rate of change} \\ \text{of muscle} \\ \text{fatty acid conc.}}} = \underbrace{k_A A_b}_{\substack{\text{uptake of} \\ \text{fatty acids} \\ \text{from blood}}} + \underbrace{k_T(1 + k_{TI}I)T_b}_{\substack{\text{insulin-controlled} \\ \text{uptake of triglycerides} \\ \text{from blood}}} - \underbrace{M_A A_m P}_{\substack{\text{oxidation of} \\ \text{fatty acids}}}, \tag{16}$$

$$\underbrace{\frac{dP}{dt}}_{\substack{\text{rate of change} \\ \text{of muscle} \\ \text{AMP conc.}}} = \underbrace{\mu}_{\substack{\text{production} \\ \text{of AMP}}} - \underbrace{\lambda_P P}_{\substack{\text{decay} \\ \text{of AMP}}} - \underbrace{\gamma_a M_A A_m P}_{\substack{\text{oxidation of} \\ \text{fatty acids}}} - \underbrace{\gamma_g M_G P I G_m}_{\substack{\text{oxidation of} \\ \text{glucose} \\ \text{(insulin-dependent)}}}. \tag{17}$$

We have neglected the internal reversible conversion of fatty acids into triglycerides which is equivalent to the storage of glucose as glycogen. We do not expect these effects to significantly alter the behaviour of the model, and including them would only complicate further an already involved system of equations.

The eight coupled nonlinear differential equations (10)–(17) represent the flows in Figure 1. There are 36 free parameters, which are listed in Table 1. Note that there are five flows in this diagram that are regulated by insulin. Four (namely the entry of glucose into the muscle cell, the entry of triglycerides into the cell, the production of ATP from glucose, the conversion of glucose to glycogen in the cell) have a positive dependence on insulin and one (namely the inhibition of the conversion of glycogen back into glucose) a negative dependence.

The process of determining the parameters listed in Table 1 (including references for each parameter found) was started during the study group, but not completed. Whilst important, this is a longer-term goal since, in the literature, there is debate over precise values for the parameters, and determining what data actually represent requires extensive numerical simulation, which is beyond the timescale of this write-up. Some of the data have been found in [1, 3, 4, 5, 7, 8, 9, 10, 11, 12, 15]. In Section 3, we use example data to illustrate the types of behaviour that can be exhibited by the system.

| Parameter | Description | Value |
|---|---|---|
| $M_G$ | Glucose oxidation rate constant | $0.97\text{mg kg}^{-1}\text{min}^{-1}$ |
| $M_A$ | FFA oxidation rate constant | $1.8$ or $1.1\text{mg kg}^{-1}\text{min}^{-1}$ |
| $k_Y$ | glycogen synthesis rate constant (basal) | 0 |
| $k_{YI}$ | glycogen synthesis constant (insulin stimulated) | |
| $k_{YP}$ | glycogen syntehsis constant (AMP inhibited) | |
| $k_T$ | muscle triglyceride uptake constant (basal) | |
| $k_{TI}$ | muscle triglyceride uptake const. (insulin stimulated) | 0 |
| $k_G$ | muscle glucose uptake constant (basal) | $18.6\mu\text{mol/kg muscle/min}$ |
| $k_{GI}$ | muscle glucose uptake constant (insulin stimulated) | |
| $k_{CP}$ | glycogenolysis constant (AMP stimulated) | |
| $k_{CI}$ | glycogenolysis constant (insulin inhibited) | |
| $S_A$ | body FFA consumption rate (release pre+post feed) | $1/3/\text{hr}=10\mu\text{mol/kg body}$ |
| $S_G$ | body glucose consumption rate | |
| $S_T$ | body triglyceride consumption rate | $13.9$ mg/h |
| $\mu$ | AMP (P) creation rate | $([\text{AMP}] = 0.1 - 6 \ \mu \text{ M})$ |
| $\lambda_I$ | insulin degradation rate | plasma $\frac{1}{2} = 6$ mins |
| $k_{IG}$ | insulin production rate | |
| $k_{IA}$ | insulin production rate | |
| $k_A$ | muscle FFA uptake rate constant | |
| $\beta_A$ | basal FFA production rate | |
| $\beta_T$ | basal triglyceride production rate | |
| $\beta_G$ | basal glucose production rate | $2.7$ mg/kg/min |
| $\tau_A$ | delay from feeding to FFA reaching blood plasma | 3 hrs |
| $\tau_T$ | delay from feeding to triglycerides reaching blood | 3 hrs |
| $\tau_G$ | delay from feeding to glucose reaching blood plasma | 10 mins |
| $k_{FA}$ | rate of uptake of FFA to blood | $2/3 \text{ hr}^{-1}$ |
| $k_{FG}$ | rate of uptake of glucose to blood | $1/3 \text{ hr}^{-1}$ |
| $k_{FT}$ | rate of uptake of triglycerides to blood | $\text{hr}^{-1}$ |
| $\theta_G$ | amount of carbohydrates in diet | 0.55 |
| $\theta_A$ | amount of FFA in diet | 0.15 |
| $\theta_T$ | amount of triglyceride in diet | 0.15 |
| $F$ | total calorific content of diet | |
| $\alpha$ | plasma volume/skeletal muscle volume | 0.17 |
| $\gamma_a$ | number of P molecules used when FFA is oxidised | |
| $\gamma_g$ | number of P molecules used when glucose is oxidised | 32 |
| $\lambda_P$ | degradation of P in absence of any other process | |

Table 1: Summary of parameters in the model.

## 2.2 The steady-state

At large-times, by which we mean about 12 hours after a meal, the functions $F_G$, $F_A$ and $F_T$ in (7)–(9) approach the constants $\beta_G$, $\beta_A$ and $\beta_T$ respectively. The equations (10)–(17) then have a steady-state solution. We denote steady-state values by a superscript '*'.

We first solve (10)–(12) to find

$$A_b^* = \frac{\beta_A}{k_A + S_A}, \qquad T_b^* = \frac{\beta_T}{S_T + k_T(1 + k_{TI}I^*)}, \qquad G_b^* = \frac{\beta_G}{S_G + k_G(1 + k_{GI}I^*)}. \qquad (18)$$

Equation (13) is a quadratic which determines the insulin level; this has the solution

$$I^* = \frac{1}{2\lambda k_G k_{GI}} \left( -b_i + \sqrt{b_i^2 + 4\lambda k_G k_{GI} c_i} \right), \qquad (19)$$

where

$$b_i = \lambda(S_G + k_G) - \frac{k_{IA}\beta_A k_G k_{GI}}{k_A + S_A}, \qquad c_i = k_{IG}\beta_G + \frac{k_{IA}\beta_A(S_G + k_G)}{k_A + S_A}. \qquad (20)$$

Since the quadratic has the form $\lambda k_G k_{GI} I^2 + b_i I - c_i$ with $\lambda k_G k_{GI} c_i > 0$ the two roots are both real, with one being positive (19) and the other negative.

The system can thus be decoupled into two subsystems which can be solved independently: one for $G_b$, $A_b$, $T_b$, $I$ whose solution drives the secondary system for $A_m$, $G_m$, $Y_m$ and $P$. The equations (14)–(16) for $G_m$, $Y_m$, $A_b$ are solved next, with solutions

$$G_m^* = \frac{\beta_G k_G(1 + k_{GI}I^*)}{M_G P^* I^*(S_G + k_G(1 + k_{GI}I^*))}, \qquad (21)$$

$$Y_m^* = k_Y G_m \left( \frac{1 + k_{YI}I^*}{1 + k_{YP}P^*} \right) \left( \frac{1 + k_{CI}I^*}{k_{CP}P^*} \right), \qquad (22)$$

$$A_m^* = \frac{1}{P^* M_A} \left[ \frac{k_A \beta_A}{k_A + S_A} + \frac{\beta_T k_T(1 + k_{TI}I^*)}{S_T + k_T(1 + k_{TI}I^*)} \right]. \qquad (23)$$

All these can be substituted into (17) to find

$$P^* = \frac{\mu - \mu_c}{\lambda_P}, \qquad \mu_c := \frac{\gamma_G \beta_G k_G(1 + k_{GI}I^*)}{S_G + k_G(1 + k_{GI}I^*)} + \frac{\gamma_A \beta_A k_A}{k_A + S_A} + \frac{\gamma_A \beta_T k_T(1 + k_{TI}I^*)}{S_T + k_T(1 + k_{TI}I^*)}. \qquad (24)$$

Since all these variables are concentrations, they must be positive, and to ensure that $P^* > 0$, we are left with the constraint $\mu > \mu_c$, where $\mu_c$ is defined in (24), and $I^*$ is given by (19)–(20).

We are fortunate indeed that, given such a complicated system of equations, it is possible to find a steady-state solution in explicit form, and furthermore, through the process of direct solution, to show that such a state is unique.

## 2.3 Non-dimensionalisation

Before attempting a numerical solution of the equations (10)–(17) to investigate the kinetics of the system following a meal, we nondimensionalise the equations. To nondimensionalise the system, we rescale each variable by its steady-state value (18)–(24), and introduce new, nondimensional, variables denoted with hats, *via*

$$\widehat{G}_b = \frac{G_b}{G_b^*}, \quad \widehat{A}_b = \frac{A_b}{A_b^*}, \quad \widehat{T}_b = \frac{T_b}{T_b^*}, \quad \widehat{I} = \frac{I}{I^*}, \tag{25}$$

$$\widehat{G}_m = \frac{G_m}{G_m^*}, \quad \widehat{Y}_m = \frac{Y_m}{Y_m^*}, \quad \widehat{A}_m = \frac{A_m}{A_m^*}, \quad \widehat{P} = \frac{P}{P_b^*}, \quad t = \frac{\alpha G_b^*}{\beta_G} \widehat{t}. \tag{26}$$

We choose the timescale to be that of the equilibration of the blood glucose level ($G_b$). At large times, $F_G(t) \sim \beta_G$, so (10) has the form $\alpha \dot{G}_b = \beta_G - \beta_G G_b/G_b^*$, giving the characteristic timescale $\alpha G_b^*/\beta_G$. This is relatively fast, when compared to the rates of change of fat levels in the blood. Values for the steady-state concentrations are available in the literature, some being listed in Table 2.

| Parameter | Description | Value |
|:---:|:---|:---:|
| $G_b^*$ | plasma glucose | 85 mg/dl |
| $A_b^*$ | plasma FFA | 140 $\mu$M |
| $T_b^*$ | plasma triglyceride | 68 mg/dl |
| $I$ | plasma insulin | 10 $\mu$U/ml or 72 mIU/l |
| $Y_m^*$ | fasted muscle glycogen content | 68 $\mu$M or 80 nmol/l muscle |
| | muscle TG | 50 mmol/kg dry weight |
| $G_m^*$ | muscle glucose | |
| $A_m^*$ | muscle FFA | |
| $P^*$ | muscle AMP | |

Table 2: Values of steady-state concentrations determined from published experimental data. The insulin units can be converted to standard dimensions by noting that 1 $\mu$mol per ml = 1 mmol per l = 6 pmol per l. We expect a larger value for the glycogen content. Also, this should be quoted in units of mmol of glucose equivalent per kg fresh weight. Hopefully a more detailed search of the literature will yield such a value.

The forcing functions $F_G(t)$, $F_A(t)$ and $F_T(t)$ and their associated parameters are nondimensionalised as follows

$$\widehat{F}_G\left(\widehat{t}\right) = 1 + \frac{\widehat{k}_{FG}\widehat{t}}{\widehat{\tau}_G} e^{-\widehat{t}^2/2\widehat{\tau}_G^2}, \qquad \widehat{k}_{FG} = \frac{F\theta_G}{B_G\beta_G}, \qquad \widehat{\tau}_G = \frac{B_G\beta_G}{\alpha G_b^*}, \tag{27}$$

$$\widehat{F}_A\left(\widehat{t}\right) = 1 + \frac{\widehat{k}_{FA}\widehat{t}}{\widehat{\tau}_A} e^{-\widehat{t}^2/2\widehat{\tau}_A^2}, \qquad \widehat{k}_{FA} = \frac{F\theta_A}{B_A\beta_A}, \qquad \widehat{\tau}_A = \frac{B_A\beta_G}{\alpha G_b^*}, \tag{28}$$

$$\widehat{F}_T\left(\widehat{t}\right) = 1 + \frac{\widehat{k}_{FT}\widehat{t}}{\widehat{\tau}_T} e^{-\widehat{t}^2/2\widehat{\tau}_T^2}, \qquad \widehat{k}_{FT} = \frac{F\theta_T}{B_T\beta_T}, \qquad \widehat{\tau}_T = \frac{B_T\beta_G}{\alpha G_b^*}. \tag{29}$$

Here we note that $\theta_G$, $\theta_A$, $\theta_T$ are already nondimensional, being proportions of the diet composed of carbohydrates, fatty acids and triglycerides respectively. The $\theta_*$ values do not sum to one since typical diets include significant amounts of protein, which we are neglecting in the current model.

We obtain the nondimensional equations (in which, for convenience, we have dropped the hats on the variables)

$$\frac{\mathrm{d}G_b}{\mathrm{d}t} = F_G - G_b + \beta_0 G_b(1 - I), \tag{30}$$

$$\epsilon_{ab}\frac{\mathrm{d}A_b}{\mathrm{d}t} = \psi_a(F_A - A_b), \tag{31}$$

$$\epsilon_t\frac{\mathrm{d}T_b}{\mathrm{d}t} = \psi_T(F_T - T_b) + \gamma_t\beta_4(1 - I)T_b, \tag{32}$$

$$\epsilon_i\frac{\mathrm{d}I}{\mathrm{d}t} = \beta_6(G_b - I) + \beta_7(A_b - I), \tag{33}$$

$$\epsilon_g\frac{\mathrm{d}G_m}{\mathrm{d}t} = \mu_g(G_b - PIG_m) - \beta_0 G_b(1 - I)$$
$$- \beta_2\left(\frac{(1+\gamma_p)}{(1+\gamma_p P)}\frac{(1+\gamma_y I)}{(1+\gamma_y)}G_m - \frac{(1+\gamma_I)}{(1+\gamma_I I)}PY_m\right), \tag{34}$$

$$\epsilon_{am}\frac{\mathrm{d}A_m}{\mathrm{d}t} = \mu_a(A_b - A_m P) - \beta_4(A_b - T_b + \gamma_t(A_b - IT_b)), \tag{35}$$

$$\epsilon_y\frac{\mathrm{d}Y_m}{\mathrm{d}t} = \beta_2\left(\frac{(1+\gamma_p)}{(1+\gamma_p P)}\frac{(1+\gamma_y I)}{(1+\gamma_y)}G_m - \frac{(1+\gamma_I)}{(1+\gamma_I I)}PY_m\right), \tag{36}$$

$$\epsilon_p\frac{\mathrm{d}P}{\mathrm{d}t} = \mu_p(1 - P) + \gamma_g\mu_g P(1 - IG_m) + \gamma_a\mu_a P(1 - A_m). \tag{37}$$

Here, the new (dimensionless) parameters are given by

$$\beta_0 = \frac{k_G k_{GI} I^* G_b^*}{\beta_G}, \quad \beta_2 = \frac{k_{CP} P^* Y_m^*}{\beta_G(1 + k_{CI} I^*)}, \quad \beta_4 = \frac{k_T T_b^*}{\beta_G}, \quad \beta_6 = \frac{k_{IG} G_b^*}{\beta_G}, \quad \beta_7 = \frac{k_{IA} A_b^*}{\beta_G}, \tag{38}$$

$$\gamma_p = k_{YP} P^*, \quad \gamma_I = k_{CI} I^*, \quad \gamma_y = k_{YI} I^*, \quad \gamma_t = k_{TI} I^*, \tag{39}$$

$$\mu_p = \frac{\mu}{\beta_G}, \quad \mu_g = \frac{M_G P^* I^* G_m^*}{\beta_G}, \quad \mu_a = \frac{M_A P^* A_m^*}{\beta_G}, \quad \psi_a = \frac{\beta_A}{\beta_G}, \quad \psi_T = \frac{\beta_T}{\beta_G}, \tag{40}$$

$$\epsilon_{ab} = \frac{A_b^*}{G_b^*}, \quad \epsilon_t = \frac{T_b^*}{G_b^*}, \quad \epsilon_g = \frac{G_m^*}{\alpha G_b^*}, \quad \epsilon_{am} = \frac{A_m^*}{\alpha G_b^*}, \quad \epsilon_y = \frac{Y_m^*}{\alpha G_b^*}, \quad \epsilon_p = \frac{P^*}{\alpha G_b^*}, \quad \epsilon_i = \frac{I^*}{\alpha G_b^*}, \tag{41}$$

the last line defines the various timescales relative to the timescale for the rate of change of the blood glucose concentration ($G_b$). We note that only insulin responds on a faster timescale ($\epsilon_i < 1$ while all the other $\epsilon_*$ parameters are greater than unity). The values adopted for the non-dimensional parameters are given in Table 3. Here we have introduced an additional, nondimensional, parameter, $\sigma$, which describes the insulin sensitivity. Several other parameters depend on $\sigma$, and changing the single parameter $\sigma$ allows us to alter the sensitivity of the processes which depend on insulin, and hence model the response of individuals with a variety of insulin sensitivities.

| Parameter | Value | Description |
|:---:|:---:|:---|
| $\sigma$ | 1 | Insulin sensitivity ($\sigma < 1$ for insulin-insensitive) |
| $\beta_0$ | 0.1 | Insulin-controlled takeup of glucose from plasma to cells |
| $\beta_2$ | 1 | Rate of glucose-glycogen conversion |
| $\beta_4$ | $0.001\sigma$ | Insulin-activated rate of transport of TG into muscle cells |
| $\beta_6$ | $0.1\sigma$ | Influence of blood glucose on insulin |
| $\beta_7$ | $0.01\sigma$ | Influence of blood FFA on insulin |
| $\gamma_p$ | 1 | $P$-inhibited conversion of glucose to glycogen |
| $\gamma_I$ | 1 | Insulin-inhibition of glycogen conversion to glucose |
| $\gamma_y$ | 1 | Insulin-activated conversion of glucose into glycogen |
| $\gamma_t$ | 0 | Insulin-controlled takeup of plasma triglyceride into muslce |
| $\mu_p$ | 4000 | Rate of AMP creation |
| $\mu_g$ | 0.3 | Rate of glucose oxidation |
| $\mu_a$ | 0.5 | Rate of FFA oxidation |
| $\psi_a$ | $0.1\sigma$ | Rate of uptake of FFA by muscle cells |
| $\psi_T$ | $0.1\sigma$ | Rate of uptake of triglyceride by muscle cells |
| $\epsilon_{ab}$ | 1 | Timescale for the evolution of blood fatty acids |
| $\epsilon_t$ | 1 | Timescale for the evolution of plasma triglycerides |
| $\epsilon_g$ | $6/\sigma$ | Timescale for the evolution of muscle glucose |
| $\epsilon_{am}$ | 1 | Timescale for the evolution of muscle fatty acids |
| $\epsilon_y$ | $60/\sigma$ | Timescale for the evolution of glycogen |
| $\epsilon_p$ | $1/\sigma$ | Timescale for the evolution of AMP |
| $\epsilon_i$ | $0.01/\sigma$ | Timescale for the evolution of insulin |
| $\gamma_a$ | 30 | Number of P molecules used when FFA is oxidised |
| $\gamma_g$ | 30 | Number of P molecules used when glucose is oxidised |
| $\widehat{\tau}_G$ | 0.5 | timescale for digestion of glucose |
| $\widehat{\tau}_A$ | 2 | timescale for digestion of FFA |
| $\widehat{\tau}_T$ | 2 | timescale for digestion of triglycerides |
| $\widehat{k}_{FG}$ | 120 | nondimensional quantity of carbohydrate ingested |
| $\widehat{k}_{FA}$ | 150 | nondimensional quantity of FFA ingested |
| $\widehat{k}_{FT}$ | 100 | nondimensional quantity of triglycerides ingested |

Table 3: List of nondimensional parameters, their interpretation, and values used to produce the example results illustrated in Section 3. Note that timescales are measured relative to the timescale for the evolution of the blood glucose level.

## 2.4   Constraints

The set of dimensionless parameter definitions (38)–(41) may not be optimal in terms of reducing the number of parameters, but many of them are calculable from data published in the literature.

The system of equations (30)–(37) highlights various additional constraints on the parameters. Let us first consider equation (30). If $I$ were to be small and $F_G$ constant, we would still expect the blood glucose concentration $G_b$ to approach a steady value.

Similarly, in equation (32), with $F_T$ constant and $I$ small, the system should asymptote to a steady value of $T_b$. Hence we expect

$$\beta_0 < 1, \qquad \text{and} \qquad \psi_T > \gamma_t \beta_4. \tag{42}$$

The former simply implies that the steady-state supply of glucose into the bloodstream should be larger than the insulin-controlled uptake rate from the bloodstream into muscle cells. The latter implies that the supply of triglycerides from adipose tissue into the bloodstream should be larger than the insulin-controlled uptake into muscle cells.

We still expect there to be a flow of glucose and fat from the bloodstream to the muscle in order for the cells to have sufficient energy to stay alive and convert AMP to ATP. From the top line of equation (34), for this to happen when $I = 0$, we require

$$\mu_g > \beta_0; \qquad \text{moreover,} \qquad \mu_a > \beta_4(1 + \gamma_t) \tag{43}$$

arises in a similar fashion by considering the terms involving $A_b$ in equation (35). Since as $t \to \infty$, the fluxes of glucose and lipids through the network in Figure 1 do not decay to zero, the resultant state can only be described as steady, and not an equilibrium.

From (37), requiring the steady-state $P = 1$ to be stable leads to

$$\mu_p > \gamma_g \mu_g + \gamma_a \mu_a, \tag{44}$$

this prevents the possibility of a blow-up in $P$ if $A_m$ and/or $G_m$ are below their steady-state values. Physically this implies that the production rate of $P$ should exceed the sum of the destruction rates due to glucose and fatty acid oxidation.

## 2.5   Assessing metabolic flexibility

To consider metabolic flexibility, we need to measure how large a switch between glucose oxidation and fatty acid oxidation can be achieved. Hence we define a quantity

$$S_W = \frac{\mu_g P I G_m}{\mu_a A_m P + \mu_g P I G_m} = \frac{\mu_g I G_m}{\mu_a A_m + \mu_g I G_m}, \tag{45}$$

which is the proportion of oxidation due to glucose. Clearly $0 \leq S_W \leq 1$. Since in (37), we expect $\gamma_g \mu_g > \gamma_a \mu_a$, when glucose levels are high, we expect insulin levels also to be high, and so the system will burn glucose at a much faster rate than fatty acids, leading to high levels of $S_W$, that is, values near one. However, when glucose levels fall, we also expect insulin to return to its level of the fasted state, and fatty acid oxidation will then dominate, leading to small values of $S_W$. The magnitude of the switch between the highest level of $S_W$ and the lowest is a measure of flexibility. In insulin insensitive individuals, we expect to observe considerable fatty acid oxidation even when glucose levels are high, leading to a lower maximum value of $S_W$ than in insulin-sensitive ones.

Experimentally, metabolic flexibility is measured using $\Delta RQ|_{\text{clamp}}$ measurements. The respiratory quotient ($RQ$) is the ratio of $CO_2$ production to $O_2$ consumption. Under

conditions of entirely carbohydrate oxidation, $RQ = 1$, whereas pure fatty acid oxidation yields $RQ = 0.71$; (these figures ignore protein and amino acid oxidation). A dose of insulin will cause a rise in $RQ$ as it allows glucose to be oxidised. The rise in $RQ$ is recorded as $\Delta RQ$. $RQ$ can exceed unity, if respiration is accompanied by the conversion of carbohydrates into fats, and $RQ$ can drop below 0.7 in starvation.

# 3    Results of numerical simulations

The results of our numerical simulations are illustrated in Figures 2 – 4. Due to the current lack of data for parameters, all graphs show nondimensional quantities, in which concentrations are measured in multiples of their steady-state values in the fasted state. However, it is useful to note the timescales of interest. The timescales are chosen to illustrate both the kinetics of the short-term post-prandial state, and the longer-term return to the fasted state which occurs over several hours. From (26) we know that one hour corresponds to nondimensional time unit of $\beta_G/\alpha G_b^*$. We take data from an average human male, weighing 70kg, and having 4.5 litres of blood. Now $\alpha = 1/6$ (dimensionless), $G_b^* = 85$ mg / dl (Table 2) giving $G_b^* =3885$ mg per person, and $\beta_G = 2.7$ mg/kg/min which is equivalent to $\beta_G = 11340$ mg per person per hr. Hence $t =$ one hour corresponds to $\widehat{t} = 11340*6/3885 = 17.5$; $\widehat{t} = 10$ corresponds to 34 minutes and $\widehat{t} = 100$ to 5.7 hours.
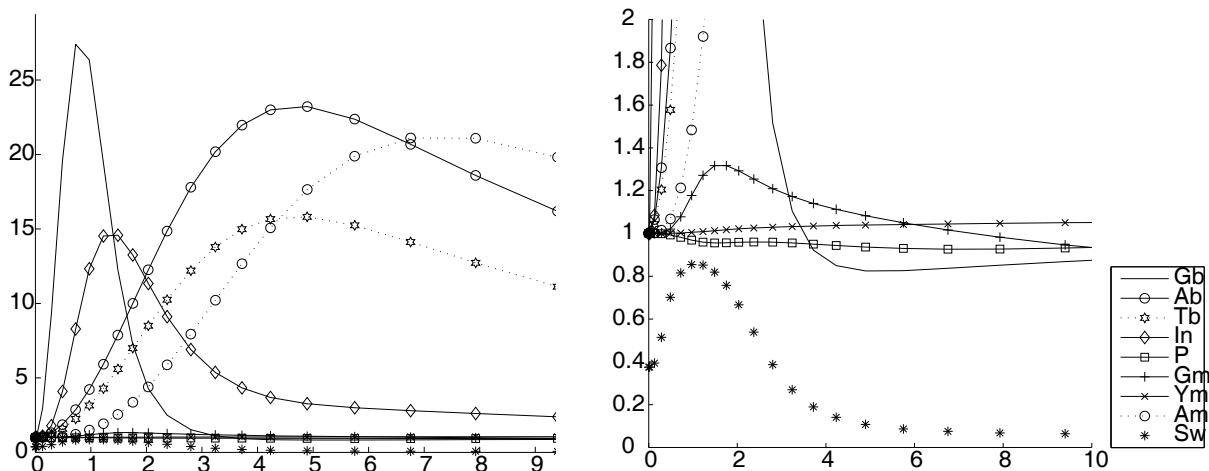


Figure 2: Short-timescale post-prandial kinetics. All nondimensional concentrations are plotted against time, on left: unconstrained ranges on the vertical axis; on right, vertical axis constrained to $0 \leq x \leq 2$ to show more clearly the behaviour near to the steady-state. A nondimensional time of $\widehat{t} = 10$ corresponds to 34 minutes.

Figure 2 shows that over the short time-scale of a few minutes the blood glucose and insulin levels rise in response to the carbohydrate in the meal. Whilst the blood glucose concentration drops back and below its steady-state level, the insulin level remains elevated since it also responds to the fatty acid which, along with the triglycerides, enters the blood plasma over a timescale of about an hour. The muscle glucose $(G_m)$ and muscle fatty acid $(A_m)$ concentrations follow the plasma glucose $(G_b)$ and plasma fatty acid $(A_b)$

ones respectively, both being delayed versions and showing a lower amplitude. For the parameter values used here we see little deviation of the glycogen concentration ($Y_m$) from its steady value.
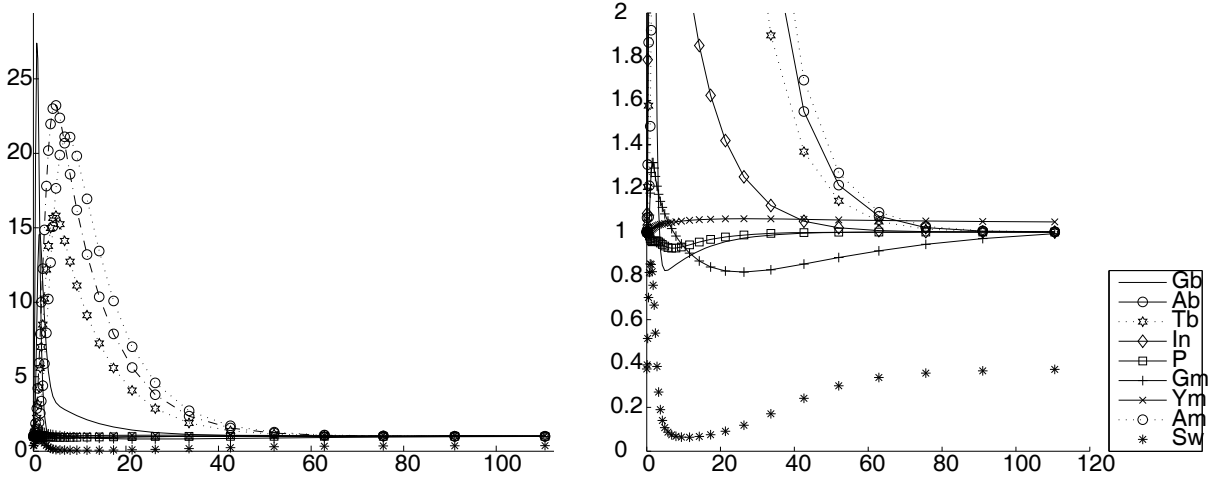


Figure 3: Longer-term post-prandial kinetics, showing return to the fasted steady-state. All nondimensional concentrations are plotted against time. Left: unconstrained ranges on the vertical axis; right: vertical axis constrained to $0 \leq x \leq 2$ to show more clearly the behaviour near to the steady-state. A nondimensional time of $\hat{t} = 100$ corresponds to 5.7 hours.

The right-hand graph in Figure 2 shows $P$ oscillating first in response to the glucose spike and later in response to the fatty acid surge. The longer-term dynamics as the system returns to its steady-state are shown in Figure 3. The switching variable $S_W$ defined in (45) is the proportion of $P$ which is oxidised by glucose (the bottom left-hand pathway in Figure 1) as opposed to the fatty-acid pathway (bottom right). The dependence of $S_W$ on insulin sensitivity is analysed in more detail in the next section.

## 3.1   Examples of insulin sensitivity

We show that by varying some of the parameters so as to more closely reflect a patient with diabetes, via the associated insensitivity to insulin, we obtain less dramatic changes in the switching parameter. This is performed by varying the parameter $\sigma$ which, from Table 3, influences the values of $\beta_4$, $\beta_6$, $\beta_7$, $\psi_a$, $\psi_T$, $\epsilon_g$, $\epsilon_y$, $\epsilon_p$, $\epsilon_i$ in equations (30)–(37).

The results are shown in Figure 4. For $\sigma = 1$, corresponding to normal insulin sensitivity, we see a rapid rise as glucose oxidation predominates (when $-1 < \log t < 0$ corresponding to 1–5 minutes); over longer times (when $2 < \log t < 3$, corresponding to 30–60 minutes), we observe a severe dip as all oxidation is of fatty acids, followed by a slow return to steady-state where both glucose and fatty acids are being oxidised. A similar curve is observed for the case $\sigma = 10$, which models the (hypothetical) case of insulin supersensitivity. The only differences are that the peak and trough occur slightly earlier than the case $\sigma = 1$. When we analyse the insulin insensitive case, where $\sigma = 0.1$ or $0.3$, we observe a dramatic reduction in the height of the peak and a delay in its position

(in time); also we note that the subsequent trough is the greatly reduced in depth, occurs later in time, and is extended in duration. During the period $2 < \log t < 5$, which corresponds to 30 minutes–8.5 hours, there is only a small shift towards fatty-acid oxidation. To summarise, insulin-insensitivity causes the proportion of glucose and fatty acid oxidation to change very little in time: there is no dominance of glucose oxidation shortly after eating, and no switch to predominantly fatty acid oxidation at later times.
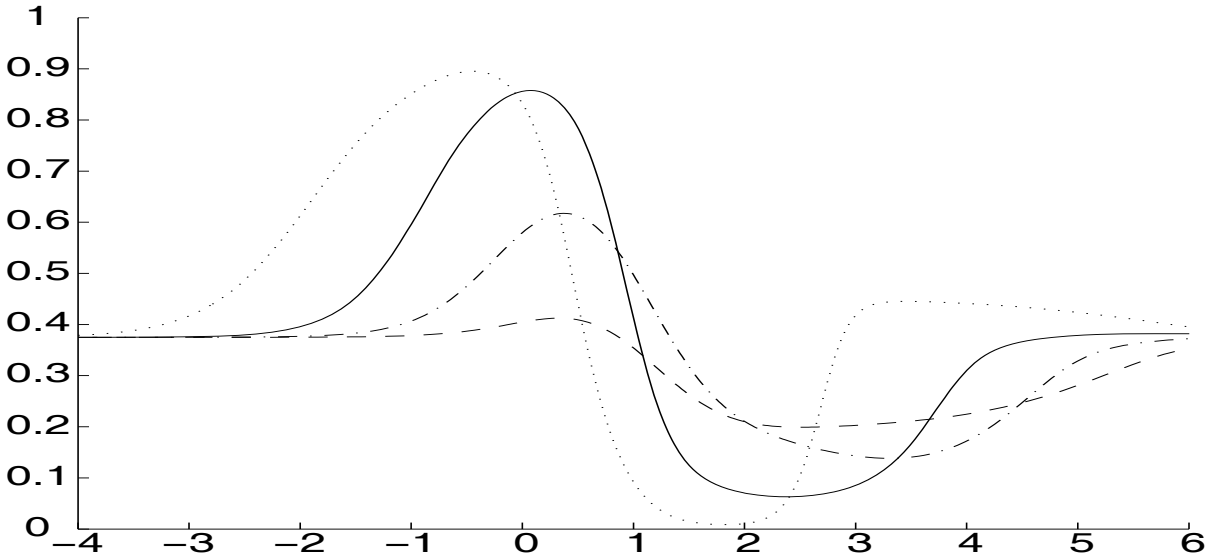


Figure 4: Plot of $S_W$ against $\log(t)$ showing the effect of varying the insulin sensitivity, $\sigma$ on the fuel switching variable $S_W$ (45). The solid line corresponds to $\sigma = 1$, the normal case; the dotted line corresponds to the insulin super-sensitive case $\sigma = 10$; the dash-dotted line to insulin insensitive case where $\sigma = 0.3$, and the dashed line to the case of extreme insulin insensitivity where $\sigma = 0.1$.

Ukropcova *et al.* [14] show fairly noisy data from the results of measurements from patients. Figure 3 of [14] plots metabolic flexibility, insulin sensitivity, body fat, and fasted insulin levels against *in vitro* adaptability. From these it is possible to construct a graph of metabolic flexibility against fasting insulin level which we could compare to our model results. Metabolic flexibility is then measured by $\Delta RQ|_{\text{clamp}}$, that is, the change in respiratory quotient, or the difference in glucose oxidation between fed and fasted states.

## 4    Conclusions

We have developed a model which exhibits switching of oxidation between glucose and fat in accordance with insulin levels as a natural consequence of the system's dynamics, without the need for an artificial switching term. Simulations using this model qualitatively reproduce experimental observations of the evolution of glucose and fat levels in blood and muscle tissue following a meal.

Appropriate future work includes:

- the need to address the role of whatever enzymes or hormones control the transport of triglycerides from the blood into fatty acids in the cell;
- a more precise description of what $P$ stands for, whether it is AMP, or an enzyme/hormone which controls the oxidation pathway;
- finding parameter values from the literature;
- validating the model against experimental data from the literature, *e.g.* Ukropcova *et al.* [14], (determining how $\Delta RQ|_{\text{clamp}}$ depends on our model variables);
- possibly including a triglyceride store for fat within the cell;
- reformulating the model in terms of calorific content rather than concentrations. This would allow a more straightforward comparison of the relative effects of glucose and fat oxidation.

## Acknowledgements

# References

[1] AST Bickerton, R Roberts, BA Fielding, L Hodson, EE Blaak, AJM Wagenmakers, M Gilbert, F Karpe & KN Frayn. Preferential uptake of dietary fatty acids in adipose tissue and muscle in the postprandial period. *Diabetes*, **56**, 168–176, (2007).

[2] EE Blaak, G Hul, C Verdich, V Stich, A Martinez, M Petersen, EFM Feskens, K Patel, JM Oppert, P Barbe, S Toubro, I Anderson, J Polak, A Astrup, IA MacDonald, D Languin, C Holst, TI Sorensen & WHM Saris. Fat oxidation before and after a high fat load in the obese insulin-resistant state. *J Clinical Endocrinology & Metabolism*, **91**, 1462–1469, (2007).

[3] GC Burdge, J Powell & PC Calder. Lack of effect of meal fatty acid composition on postprandial lipid, glucose and insulin responses in men and women aged 50–65 years consuming their habitual diets. *Br J Nutr*, **96**, 489–500, (2006).

[4] LK Dial, S Miyamoto & ER Arquilla. Modulation of $^{125}$I-insulin degradation by receptors in liver plasma membranes. *Biochem Biophys Res Comm*, **74**, 545–552, 1977.

[5] RR Henry, TP Ciaraldi, S Mudaliar, L Abrams & SE Nikoulina. Acquired defects of glycogen synthase activity in cultured human skeletal muscle cells: influence of high glucose and insulin levels. *Diabetes*, **45**, 400–407, (1996).

[6] DE Kelley. Skeletal muscle fat oxidation: timing and flexibility are everything. *J Clinical Investigation*, **115**, 1599–1702, (2005).

[7] DE Kelley & LJ Mandarino. Fuel selection in human skeletal muscle in insulin resistance. *Diabetes*, **49**, 677–683, (2000).

[8] DE Kelley, KV Williams & JC Price. Insulin regulation of glucose transport and phosphorylation in skeletal muscle assessed by PET. *Am J Physiol Endocrin Metab*, **277**, E361–E369, (1999).

[9] J Kim, GM Saidel & ME Cabrera. Multi-scale computational model of fuel homeostasis during exercise: effect of hormonal control. *Ann Biomedical Eng*, **35**, 69–90, (2007).

[10] LJ Mandarino, A Consoli, A Jain & DE Kelley. Interaction of carbohydrate and fat fuels in human skeletal muscle: impact of obesity and NIDDM. *Am J Physiol Endocrinol Metab*, **270**, E463–E470, (1996).

[11] S Normand, Y Khalfallah, C Louche-Pelissier, C Pachiaudi, JM Antoine, S Blanc, M Desage, JP Riou & M Laville. Influence of dietary fat on postprandial glucose metabolism (exogenous and endogenous) using intrinsically (13)C-enriched durum wheat. *Br J Nutr*, **86**, 3–11, (2001). Additional comment in *Br J Nutr*, **86**, 1–2, (2001).

[12] S del Prato, A Riccio, SV de Kreutzenberg, M Dorella, A Tiengo & RA deFronzo. Basal plasma insulin levels exert a qualitative but not quantitative effect on glucose-mediated glucose uptake. *Am J Physiology, Endocrinology & Metabolism*, **268**, E1089–E1095, (1995).

[13] L Storlien, ND Oakes & DE Kelley. Symposium 6: adipose tissue-liver-muscle interactions leading to insulin resistance. *Proc Nutrition Soc*, **63**, 363–368, (2004).

[14] B Ukropcova, M McNeil, O Sereda, L de Jonge, H Xie, GA Bray & SR Smith. Dynamics changes in fat oxidation in human primary myocytes mirror metabolic characteristics of the donor. *J Clinical Investigation*, **115**, 1934–1941, (2005).

[15] AM Wagner, J Ordonez-Llanos, R Arcelus, R Bonet, O Jorba, JL Sanchez-Quesada, E Alonso, J Julve & A Perez. Postprandial lipidemia is normal in non-obese type 2 diabetic patients with relatively preserved insulin secretion. *Metabolism*, **52**, 1038–1042, (2003).